

Accepted Manuscript

Separation of CO₂-N₂ gas mixtures: Membrane combination and temperature influence

Ana Fernández-Barquín, Clara Casado-Coterillo, Ángel Irabien

PII: S1383-5866(17)31756-2

DOI: <http://dx.doi.org/10.1016/j.seppur.2017.07.029>

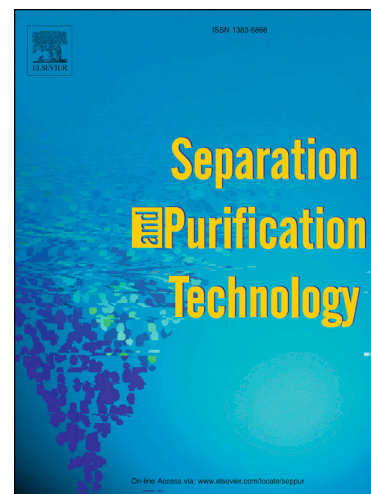
Reference: SEPPUR 13886

To appear in: *Separation and Purification Technology*

Received Date: 1 June 2017

Revised Date: 11 July 2017

Accepted Date: 11 July 2017



Please cite this article as: A. Fernández-Barquín, C. Casado-Coterillo, A. Irabien, Separation of CO₂-N₂ gas mixtures: Membrane combination and temperature influence, *Separation and Purification Technology* (2017), doi: <http://dx.doi.org/10.1016/j.seppur.2017.07.029>

This is a PDF file of an unedited manuscript that has been accepted for publication. As a service to our customers we are providing this early version of the manuscript. The manuscript will undergo copyediting, typesetting, and review of the resulting proof before it is published in its final form. Please note that during the production process errors may be discovered which could affect the content, and all legal disclaimers that apply to the journal pertain.

Separation of CO₂-N₂ gas mixtures: Membrane combination and temperature influence

Ana Fernández-Barquín¹, Clara Casado-Coterillo^{1,*}, Ángel Irabien¹

¹ *Department of Chemical and Biomolecular Engineering, Universidad de Cantabria, Av. Los Castros s/n, 39005 Santander, Spain*

*Corresponding author: casadoc@unican.es

Abstract

Novel mixed matrix membranes (MMM) with different characteristics are experimentally evaluated in a two-stage membranes-in-series bench-scale setup for the separation of CO₂-N₂ gas mixtures. For stage 1, a high permeability (higher than 1000 Barrer) and low selectivity (about 5-10) membrane is chosen: the [emim][Ac]-Chitosan (IL-CS) hybrid membrane developed in our laboratory and the Pervap 4060 (Sulzer) composite membrane. For stage 2, we chose our Zeolite A/PTMSP MMM, whose selectivity is higher than 20 even at up to 343K, the CO₂ permeability not lower than 5000 Barrer, which allows skipping the use of the intermediate compressor. The influence of membrane intrinsic properties (*i.e.* selective membrane material), number of modules in series, and feed concentration on separation performance is evaluated experimentally. In this system, a 10% CO₂ feed is concentrated to 43%, 26 and 40% for the Zeolite A/PTMSP MMM – Zeolite A/PTMSP MMM, IL-CS – Zeolite A/PTMSP and Pervap 4060 – Zeolite A/PTMSP in stage 1 and stage 2, respectively. The agreement of the experimental results with a mathematical model at the low CO₂ feed concentration of flue gas allows estimating the membrane area needed for each

membrane material to achieve a given CO₂ purity and removal efficiency. The very large membrane areas needed to reach the 90% CO₂ purity and removal efficiency target are drastically reduced if the CO₂ removal efficiency required is set to 70%, especially for the combinations with different membranes in each stage, which gives scope for attempting further development of novel membrane materials for CO₂ capture processes.

Keywords: CO₂ capture; Experimental gas separation; Mixed matrix membrane materials; Temperature; Two-stage configuration

1. Introduction

Global warming and climate change are environmental issues resulting from the rise on worldwide energy consumption that releases increasing levels of greenhouse gases to the atmosphere. The EU especially urges that technologies for the CO₂ capture from flue gases are developed to achieve the climate targets by 2030 and limit the average global temperature to 2°C [1].

Despite the research efforts dedicated to the different strategies of CO₂ capture from large emission sources such as chemical industries and power plants, it is still post-combustion the only feasible option for implementation at large scale, because it enables retrofitting [2]. The main challenges of post-combustion capture are the low CO₂ concentration, i.e. low pressure of the feed gas, and the huge gas flow rates to be treated. Nowadays, the most mature CO₂ post-combustion capture plants are based on chemical absorption with chemical solvents, usually amines. However, the high energy requirements, solvent losses by flooding, solvent deactivation or secondary CO₂ production, as well as the huge equipment requirements, make retrofitting far from real

implementation [3] and systematic materials and process research is required to intensify the post-combustion carbon capture process [4,5].

Membrane technology has been continuously studied in the last decade as a potential alternative in terms of scalability, energy saving and modularity, low capital investment, small carbon footprint and reduced energy requirement [6]. However, available gas separation membranes use at commercial scale for CO₂ capture is still limited to pilot plant studies [7–9]. The sensitivity of existing membrane materials towards harsh process conditions, such as temperature, pressure or the presence of impurities has prevented so far the development of membrane technology to high technology readiness level (TRL) and justify a worldwide search on the development of membrane materials [10] and process designs [11,12].

The main parameters that influence the choice of a gas separation membrane are the intrinsic transport properties of the membrane, *i.e.* the permeability and selectivity. Polymer membranes usually face a generally acknowledged trade-off in selectivity and permeability, defined by Robeson's upper bound [13], including blends and mixed matrix membranes (MMMs) [14]. When dealing with CO₂-N₂ gas mixture separations, the effect of operation conditions (partial pressure and feed composition) and the engineering design leading to integrate membranes in CO₂ capture (module configuration, stage cut and flow management), depend on the membrane material that provides the optimized permeability and selectivity [10,12,15]. Regarding the process design approach, simulated approaches reported state that current membranes cannot offer high purity and high CO₂ recovery at the same time in one stage due to the partial pressure driving force limitation, irrespective of the membrane selectivity and permeability [16–20].

Therefore, in order to reach with membranes the high removal efficiency and CO₂ concentration in the permeate that would allow membrane technology to be competitive with conventional processes, different multi-stage process configurations have been simulated [21]. Most simulation and optimization approaches use data from the Polaris® membrane from MTR, whose CO₂ permeance of 1000 GPU (1 GPU = 10⁻⁶ cm³(STP) · cm⁻² · s⁻¹ · cmHg⁻¹) and moderate CO₂/N₂ selectivity, at an affordable pressure ratio [22]. The selectivity loses significant if recycling to pre-concentrate the flue gas before the membrane is enabled [23]. One step further in this negligibility of the selectivity was the consideration of N₂-selective instead of CO₂ selective membranes, simulated by Yuan et al. [24], arriving to the conclusion that the feed compression required in the single stage becomes optional in the two-stage system.

Van der Sluijs et al. were the first to simulate a two-stage membrane system where different intrinsic permeability and selectivity membranes were considered for each stage. Using available data for commercial polymeric membranes, they also concluded that the two membrane system is necessary to reach a CO₂ purity over 80%, but that the single membrane stage was the most economic configuration if only a CO₂ purity lower than 70% was required. Gerber [25] patented the concept of a two-stage system combining a membrane of high permeability in the first stage and a different membrane of high selectivity in the second stage in order to improve the CO₂ capture from natural gas to reach the 90% purity target at the exit. Using a similar concept, Brunetti et al.[26] simulated the intensification of CO₂ capture from biogas by considering the intrinsic values of a Hyflon AD60 high permeability membrane material in the first stage and a high selectivity Matrimid membrane in the second stage. Actually, the development of CO₂ separation using membrane technology is more developed for natural gas than flue gas [27].

The results of all these simulations should be taken with caution since there are relatively few papers comparing them with real CO₂/N₂ mixture separation experiments at bench or pilot scale. As far as we know, the experimental evaluation of CO₂ separation from CO₂-N₂ gas mixtures has not been reported for multi-stage membrane systems [18,20,28]. This lack of demonstration of CO₂ capture from industrial plants outside simulation work implies that it is too early to identify which CO₂ capture technologies may become dominant [29].

In this work, we will use the concept of combining a high permeability and moderate selectivity membrane (permeability higher than 1000 Barrer) in stage 1 and a high selectivity (in the range 20-50) membrane in stage 2 to evaluate the CO₂/N₂ separation performance of novel membrane materials developed in our group [30,31]. In addition to the aforementioned concept, the membrane material selected for stage 2 provided high selectivity (up to 50) and high permeability even at 343 K (about 5000 Barrer), which allows avoiding the use of the intermediate compressor. The effect of the membrane combination and the number of modules, the CO₂ concentration in the feed stream and temperature has been experimentally evaluated and studied by a mathematical model. This model will then be applied to the estimation of the necessary membrane area to fabricate of each material to reach the coupled purity in the permeate and CO₂ removal efficiency established as design target.

2. Experimental

2.1. Gas separation experimental system

Gas separation experiments are carried out by means of CO₂/N₂ mixed gas separation tests using the experimental setup described elsewhere [32], and represented in Figure 1. The membrane modules consist of two parts pneumatically pressed onto

each other, where the membranes are placed on a 316LSS macro porous disk support of 20 μm nominal pore size (Mott Corp., USA) and sealed by Viton rings. The effective membrane area is 15.55 cm^2 in each module. The permeate of the stage 1, working at ambient temperature, is fed to the membrane module in stage 2 at 343 K set at a convection oven (Memmert UNE 200, Germany), without the use of a compressor between both stages.

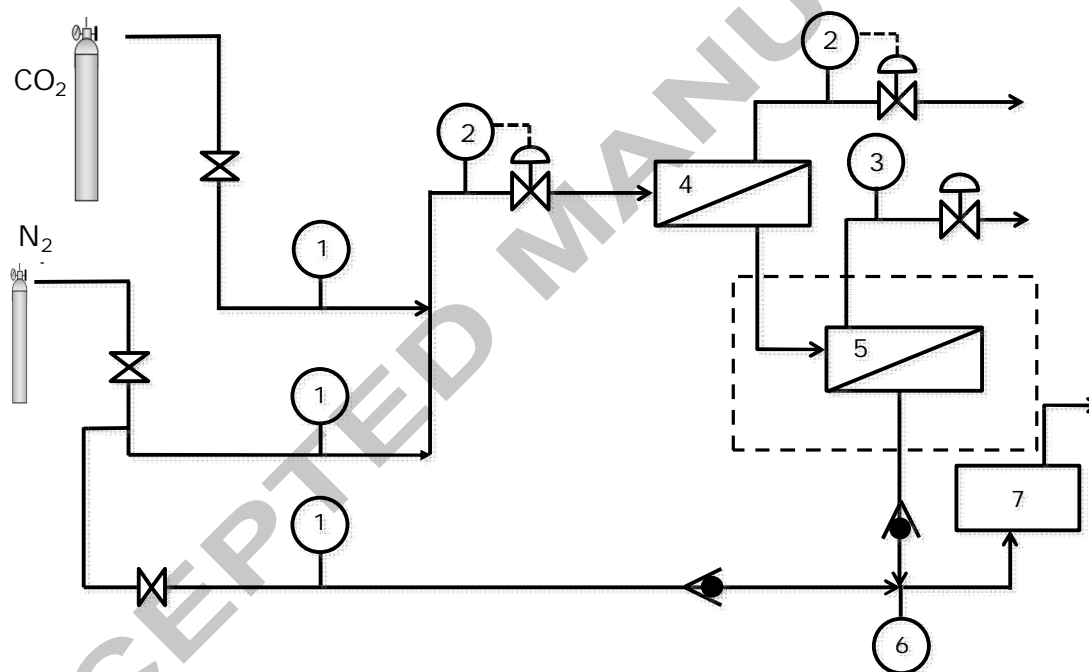


Figure 1. Experimental setup. (1) Mass flow meters, (2) pressure regulators, (3) pressure gauges, (4) module for membrane in stage 1, (5) module for membrane in stage 2, (6) bubble flowmeter and (7) CO_2 analyzer.

The feed mixture is controlled using two MC-50SCCM-D mass flow controllers (Alicat Scientific, USA) and varied from 5 to 66 CO_2 mol % in N_2 . The gases used in the experiments were carbon dioxide (99.97%) and nitrogen (>99.9999%) (Air Liquide, Spain). The pressure is regulated at the feed and retentate of the membrane modules to

generate the transmembrane pressure for separation. Pressure gauges are installed at the permeate side of stage 1 and stage 2 to measure the pressure difference in each stage. The details of the operating conditions used in the laboratory for the binary CO₂-N₂ gas mixture separation experiments simulating flue gas streams conditions are summarized in Table 1. Please note the absence of an intermediate compressor between the membrane stages in series.

Table 1. Experimental conditions in each stage of membrane modules in series. F_f is the feed flow rate, T , the operating temperature, p_f and p_r the feed and retentate pressures and ϕ_j the pressure ratio of stage j ($j = 1,2$).

	Stage 1			Stage 2		
F_f (mol/s)	T (K)	p_f (bar)	ϕ_1	T (K)	p_r (bar)	ϕ_2
$3.47 \cdot 10^{-5}$	298	3.9	1.8	343	2.1	1.7

The permeate flow rate is measured at the exit of the entire system using a bubble flow meter. The CO₂ concentration is measured by an infrared gas analyzer G100 (Fonotest, USA). The permeate stream is mixed with a N₂ flow as carrier before entering the analyzer, in the conditions given in Table 2, whose maximum CO₂ concentration is 20 %. N₂ concentration is calculated by mass balance.

Table 2. N₂ dilution flow rate for the different feed concentrations.

CO ₂ feed content [mol%]	N ₂ dilution flow rate [mol/s]
4.57	$3.46 \cdot 10^{-6}$
8.33	$6.93 \cdot 10^{-6}$

10.1	$6.93 \cdot 10^{-6}$
17.5	$6.93 \cdot 10^{-6}$
39	$6.93 \cdot 10^{-6}$
66.7	$1.04 \cdot 10^{-5}$

2.2. Membranes

The membranes selected for stage 1 are a Pervap 4060 commercial membrane with a permeability higher than 1000 Barrer and a selectivity below 10 [7], a IL-CS hybrid membrane, whose permeability is larger than 1000 Barrer and its selectivity is constant around 5 in the range of 298 – 323 K. For stage 2, a Zeolite A/PTMSP MMM developed in our laboratory, whose permeability and selectivity is larger than 5000 Barrer and 20-50, respectively, in the range 298 – 343 K. Table 3 shows the different membrane configurations evaluated in this work.

Table 3. Membrane configurations.

Single –stage system (stage 1):	Two-stage system (stage 1 + stage 2)
IL-CS	IL-CS + ZA/PTMSP
ZA/PTMSP	ZA/PTMSP + ZA/PTMSP
Commercial PDMS (Pervap4060)	Pervap 4060 + ZA/PTMSP

The mixed matrix membranes (MMM) were prepared by the solution casting method, as reported elsewhere [30,31]. The polymers were PTMSP (ABCR GmbH, Germany) and Chitosan (CS, Sigma-Aldrich Quimica S.L., Spain). Zeolite A (ZA, molecular sieves 4A, Sigma-Aldrich Quimica S.L., Spain) or the ionic liquid (IL, 1-

ethyl-3-methylimidazolium [emim][Ac]) 97%, Sigma-Aldrich Quimica S.L., Spain) were used as fillers in 20 wt.% and 5 wt.% loadings, for the ZA/PTMSP MMM and the IL-CS hybrid membrane, respectively.

The average thickness of the membranes is $128 \pm 4.0 \mu\text{m}$, $101.60 \pm 7.3 \mu\text{m}$ and $180 \pm 5.0 \mu\text{m}$ for IL-CS, ZA/PTMSP and Pervap 4060 (Sulzer GmbH, Germany) membranes, respectively.

The main assumptions considered for the mathematical model presented in Appendix A, as an initial tool for the analysis on the perspectives of new membranes in $\text{CO}_2\text{-N}_2$ separation [33], are justified below by the references in literature using them in the context of the experimental conditions employed in our laboratory (Table 1):

- The model only for a binary $\text{CO}_2\text{-N}_2$ gas mixture, which is the simplifying assumption first employed to evaluate the prediction of a multicomponent model [33,34].
- The process is considered at steady and isothermal conditions[6,12,35–38].
- The influence of temperature on the intrinsic permeability and selectivity of the membranes is stronger than that of the CO_2 concentration and pressure [39–41].
- The gases behave ideally and there is no concentration polarization, given the low pressure of the system and the thickness of the membranes involved [35,42].
- The feed side pressure drop is measured experimentally, and it is negligible since the membrane modules employed have flat geometry [17].

The parameters used in the mathematical model equations in Appendix A are summarized in Table 4. The permeability, P , and ideal selectivity, α , were measured by

single gas permeation in a constant-volume setup and reported in our previous works, as a function of temperature in the range 298 – 343 K, which allowed the determination of the activation energies given in Table 4.

Table 4. Membrane thickness, intrinsic permeability and selectivity and permeation activation energies.

Membrane	298 K		383 K		Ea(CO ₂) [kJ/mol]	Ea(N ₂) [kJ/mol]	δ [μm]
	P(CO ₂) [Barrer]	α (CO ₂ /N ₂) [-]	P(CO ₂) [Barrer]	α (CO ₂ /N ₂) [-]			
IL-CS	1,146	3.0	N.A.	N.A.	7.09	2.78	128 ± 4
ZA/PTMSP	10,184[39]	25	32,493	60	5.34	20.21	101.6 ± 7
Pervap 4060	47,376	10	N.A.	N.A.	3.04	18.9	180 ± 5

N.A.: Not Available.

The permeability, P , and ideal selectivity, α , were measured by single gas permeation in a constant-volume setup and reported in our previous works, as a function of temperature in the range 298 – 343 K, which allowed the determination of the activation energies given in Table 4.

4. Results and discussion

Table 5 collects the experimentally obtained values for permeate flux, concentration and CO₂ removal efficiency at each stage over the entire CO₂ feed composition under study, in terms of CO₂ purity and CO₂ recovery at the exit, for stage 1, stage 2 and the global system, as evaluated experimentally in the bench-scale pilot plant schematized in Figure 1 above.

ACCEPTED MANUSCRIPT

Table 5. CO₂/N₂ separation performance using different membrane material combined in a two-stage membrane system different contents of CO₂ in feed.

Stage 1	Stage 2	Stage 1			Stage 2		Global	
		Feed CO ₂ [mol%], x _f	Permeate CO ₂ [mol%], y ₁	Efficiency [%], e ₁	Permeate CO ₂ [mol %], y ₂	Efficiency, e ₂ [%]	Removal efficiency [%], e	CO ₂ flux [mol/m ² ·h]
IL-CS	ZA/PTMSP	4.57	6	28	10	31	9	0.38
		8.33	10	26	20	56	15	0.86
		10.10	13	18	26	49	9	1.17
		17.50	21	17	40	44	8	1.28
		38.89	48	17	64	35	6	2.24
		65.63	75	16	97	45	12	7.42
ZA/PTMSP	ZA/PTMSP	4.57	10	23	17	38	9	0.38
		8.33	18	30	37	58	18	0.95
		10.10	22	30	43	33	10	1.41
		17.50	33	32	52	28	9	1.50
		38.89	58	42	83	22	9	3.39
		65.63	79	39	99	29	11	7.22
Pervap 4060	ZA/PTMSP	4.57	9	18	17	51	9	0.40
		8.33	18	19	38	61	11	0.91
		10.10	21	20	40	64	13	1.25
		17.50	37	23	52	36	8	1.39
		38.89	68	30	86	29	9	3.29
		65.63	88	38	99	31	12	7.36

The feed stream with a CO₂ content of 10% is enriched to a CO₂ concentration in the permeate of 26% (IL-CS – ZA/PTMSP), 43 % (Zeolite A/PTMSP – ZA/PTMSP) and 64% (Pervap 4060 – ZA/PTMSP).

From Table 5, the ZA/PTMSP – ZA/PTMSP and Pervap 4060 – ZA/PTMSP configurations allow higher CO₂ purity at the exit of stage 2 regardless the feed concentration and IL-CS – ZA/PTMSP and Pervap 4060 – ZA/PTMSP configurations give a slightly higher global CO₂ removal efficiency. The CO₂ removal efficiency by each membrane stage j ($j = 1,2$) has been calculated by Eq. (1), and the global removal efficiency of the whole system, e , is described by Eq. (2).

$$e_j = \frac{\theta_j \cdot y_j}{x_{jf}} \quad (1)$$

$$e = \frac{\theta_1 \cdot \theta_2 \cdot y_2}{x_f} \quad (2)$$

The CO₂ removal efficiency obtained at a 10% CO₂ concentration in the feed is 13% (Pervap 4060 – ZA/PTMSP). The global CO₂ concentration in the permeate is between 64 % (IL-CS – ZA/PTMSP) to 86% CO₂ (ZA/PTMSP – ZA/PTMSP), for 50:50wt% feed mixtures of CO₂-N₂ only varying the membrane in the stage 1. As expected, in the case with the lowest CO₂ content in the feed stream (4.6 %), the permeate enrichment is the lowest, because the lower CO₂ content in the feed the lower the partial pressure and driving force through the membrane. This agrees with the well-known fact that membranes perform most efficiently when the concentration of the target component in the feed is high [36,43].

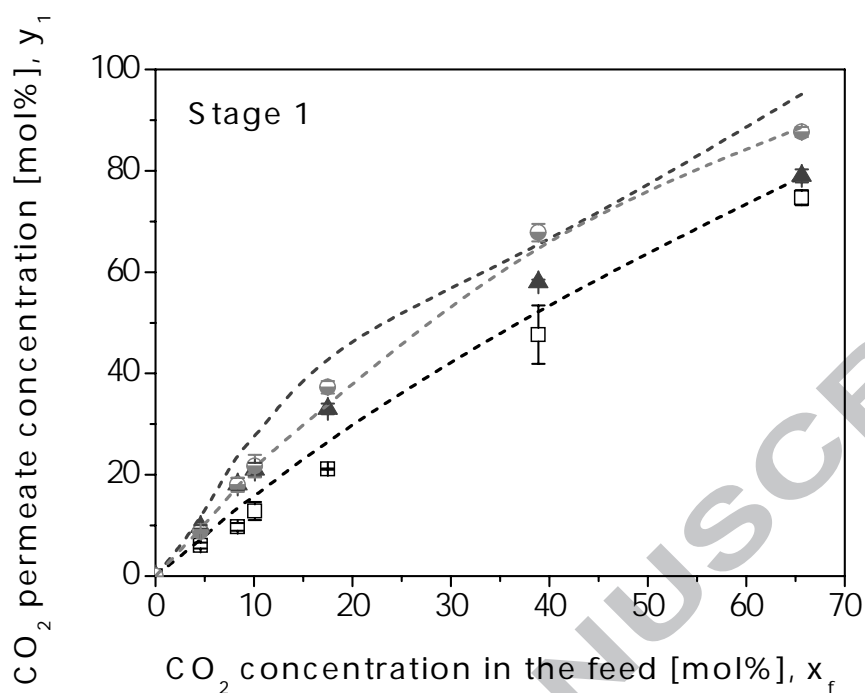


Figure 3. Comparison of experimental and model predicted CO₂ permeate concentration from stage 1, versus CO₂ concentration in the feed for the different configurations under study: IL-CS - ZA/PTMSP (void black squares), ZA/PTMSP – ZA/PTMSP (filled dark gray triangles) and Pervap 4060 - ZA/PTMSP (half-filled gray circles).

As expected, the performance of a membrane material in one stage configuration is enhanced by the incorporation of a second membrane stage [44].

From Figure 3, as the CO₂ concentration in the feed increases, the concentration in the permeate increases and the enrichment in one stage agrees with literature. For instance, Lin et al. [8] reported a CO₂ enrichment in a single stage membrane system from 9 to 33% using the Polaris® membrane. The shape of the curves in Figure 3 indicates that the type of membrane material (rubbery PDMS, semi-crystalline IL-CS or amorphous PTMSP –based membranes) influences the membrane performance. In

Figure 4, the CO₂ concentration of the permeate from stage 2 increases with increasing the CO₂ concentration coming from stage 1.

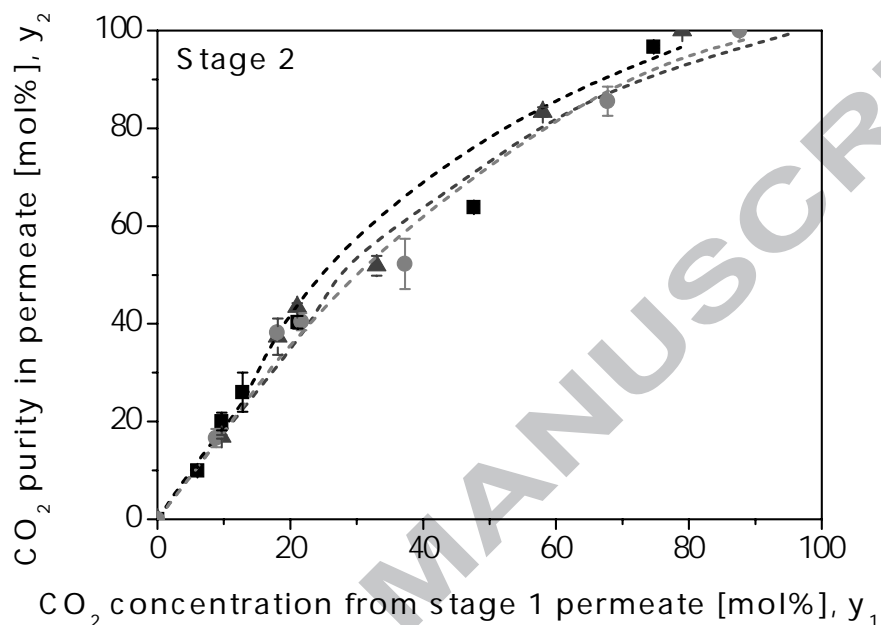


Figure 4. Comparison of experimental and model predicted CO₂ concentration of the permeate of the stage 2, versus CO₂ concentration in the permeate of the stage 1 for the different configurations under study: IL-CS – ZA/PTMSP (black squares), ZA/PTMSP-ZA/PTMSP (dark gray triangles) and Pervap 4060 – ZA/PTMSP (gray circles).

The dependence of CO₂ permeate concentration on feed concentration differed in stage 1 with the type of membrane: Pervap 4060, with a thin rubbery PDMS layer, the semi-crystalline IL-CS hybrid membrane and the ZA/PTMSP MMM (from the amorphous glassy PTMSP), as shown in Figure 3, while this difference is attenuated in the stage 2 represented in Figure 4. The only membrane used in stage 2 was the ZA/PTMSP MMM.

The experimental data obtained in one and two stages are compared in Figure 3 and Figure 4 with the model predictions (dashed lines) for the CO₂ permeate concentration in stage 1 and stage 2, respectively, versus CO₂ feed concentrations in order to characterize the different membrane systems under study. The error bands in Figure 3 and Figure 4 reflect the reproducibility of the experimental results obtained in the laboratory. The proposed model agrees acceptably well with the experimental results, with errors in the CO₂ concentration in the permeate as collected in Table 6.

Table 6. Deviation of the experiments and model predictions for the CO₂ concentration in the permeate as a function of the number of stages and membrane configurations.

	Stage 1	Stage 2
IL-CS – ZA/PTMSP	5 – 18%	18 – 23%
ZA/PTMSP – ZA/PTMSP	9 – 23%	0.7 – 16%
Pervap 4060 – ZA/PTMSP	0.5 – 8%	1.8 – 9 %

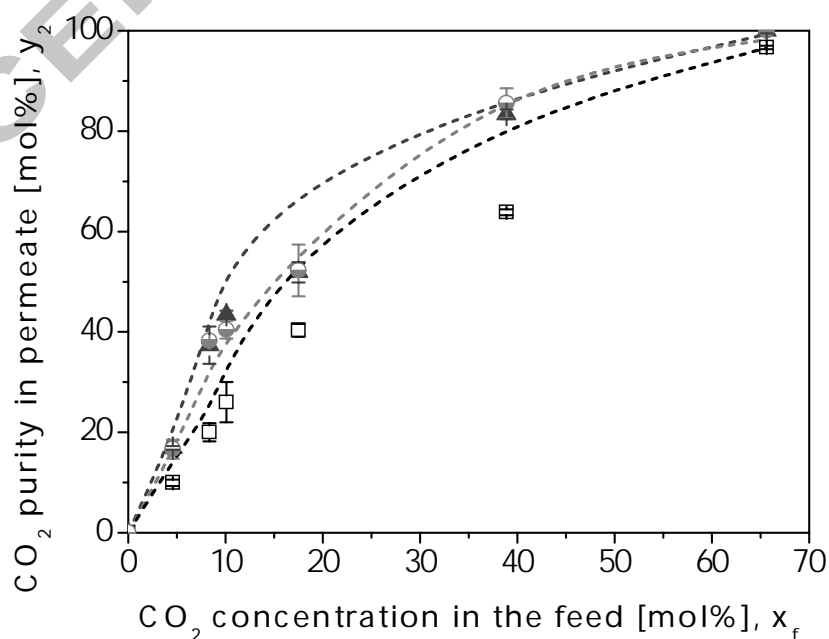


Figure 5. Experimental and simulated CO₂ permeate purity versus CO₂ concentration in the feed: IL-CS – ZA/PTMSP (void black squares), ZA/PTMSP – ZA/PTMSP (filled dark gray triangles) and Pervap 4060 – ZA/PTMSP (half-filled gray circles).

Figure 5 illustrates the effect of CO₂ concentration in the feed gas on the global permeate purity for the different two-stage membrane combinations. As expected, when the CO₂ concentration in the feed increases, the purity of the permeate increases accordingly. The trend is a combination of the dependences shown above in Figure 3 and Figure 4 for stage 1 and stage 2 separately. This agrees with the fact that at lower feed concentrations the partial pressure difference across polymer-based membranes is usually low, causing a smaller driving force through the membrane [8,45,46]. In this way, the increment in the CO₂ permeate concentration is attributed to the increasing driving force due to the increment in the CO₂ feed composition leading to higher CO₂ partial pressure [36].

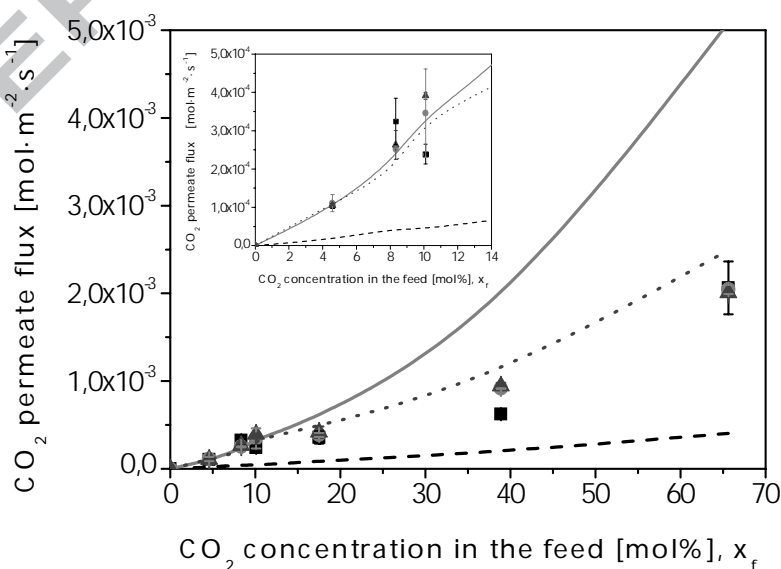


Figure 6. Comparison of experimental and simulated CO₂ permeate flux versus CO₂ concentration in the feed: IL-CS – ZA/PTMSP (black squares, dashed lines), ZA/PTMSP – ZA/PTMSP (dark gray triangles, dotted lines) and Pervap 4060 – ZA/PTMSP (gray circles, continuous lines). The area at lower CO₂ concentration in the feed is zoomed in the inset.

Figure 6 shows how the CO₂ permeate flux increases with CO₂ concentration in the feed and that the proposed model agrees with the results at low CO₂ feed concentration. At high CO₂ concentration in the feed, the model prediction only adjusts the ZA/PTMSP – ZA/PTMSP system, while the Pervap 4060 – ZA/PTMSP system is the one showing the worst agreement with the model simulation. This may be attributed to the fact that the selective layer thickness of the Pervap 4060 membrane is only 1.5 μm thick, versus the self-standing IL-CS and ZA/PTMSP MMM. Besides, there may be an antiplasticization effect due to competition between plasticization and compaction in the self-standing IL-CS or ZA/PTMSP MMM, larger than that offered by the substrate of the Pervap 4060 membrane [47–49].

The agreement between the model predictions and experimental permeation flux data, especially at low concentrations of CO₂ in the feed, allows the use of this mathematical model for a first analysis on the perspectives of new membranes in CO₂-N₂ separation [33]. The discrepancies between the model and the experimental data in CO₂ and N₂ fluxes may be attributed to the opposite influences of competitive sorption and plasticization in mixed gas separation experiments compared to single gas experiments [50], which depend on the membrane material. There is a different preferential sorption behavior of Zeolite A, the IL, and the polymers for CO₂ versus N₂ [32]. The simplifying assumptions used for this preliminary assessment are not

completely valid and the expressions including the permeability dependence on concentration should be taken into account in a future work [39,47,48,50,51].

To our knowledge this is one of the first works that study experimentally the CO₂-N₂ gas mixture separation performance of a two-stage membrane system connected in series investigating the influence of membrane materials with different intrinsic transport properties in each stage.

3.2. Application to process design

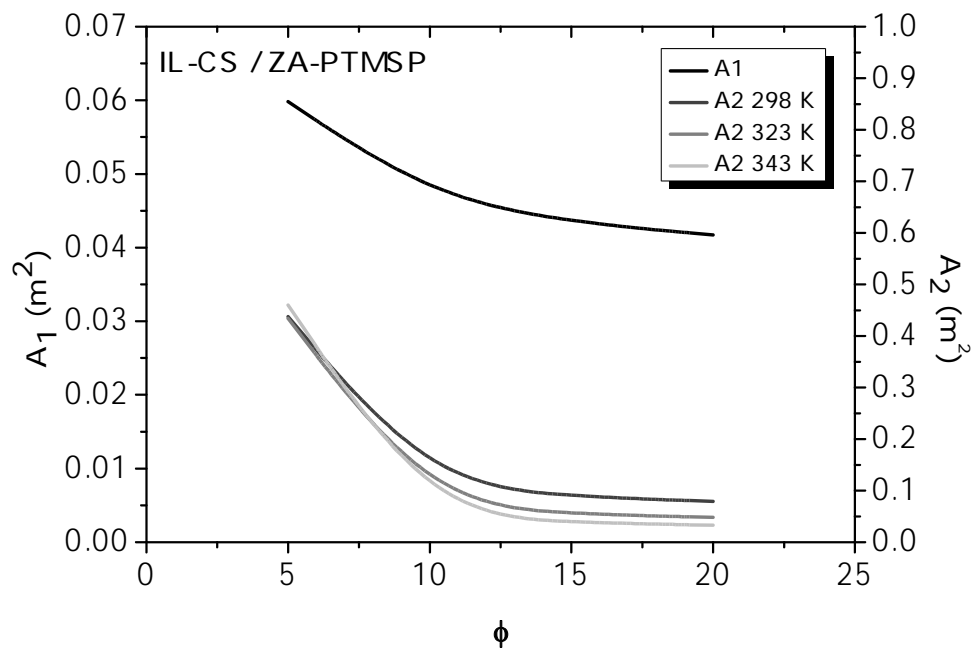
The mathematical model allows estimating the required area of each membrane material that would be necessary to achieve a certain CO₂ purity and removal efficiency, as the coupled design targets in CO₂ - N₂ separation to consider membrane technology as a potential alternative to conventional CO₂ capture methods and direct future investigations regarding membrane development and fabrication [16]. The operating conditions considered for this calculation are the same as those in Table 1.

In Figure 8, the membrane areas required for stage 1 and stage 2 of the two-stage membrane systems under study are plotted as a function of pressure ratio and temperature, for a 90% CO₂ concentration in the permeate and 90% CO₂ removal efficiency, since this is the design target usually required for membrane-based CO₂ capture processes to be competitive with chemical absorption [52]. As expected, high pressure ratios reduce the membrane area requirements but increase the energy consumption [40]. Low pressure ratio generally results in low driving force [45], existing a trade-off between the energy used to achieve the required pressure ratio and the membrane area [20]. Energy considerations will limit the maximum pressure ratio attainable by feed compression or permeate vacuum to about values of 10, which makes high membrane permeability being more important than high CO₂/N₂ selectivity [21], as

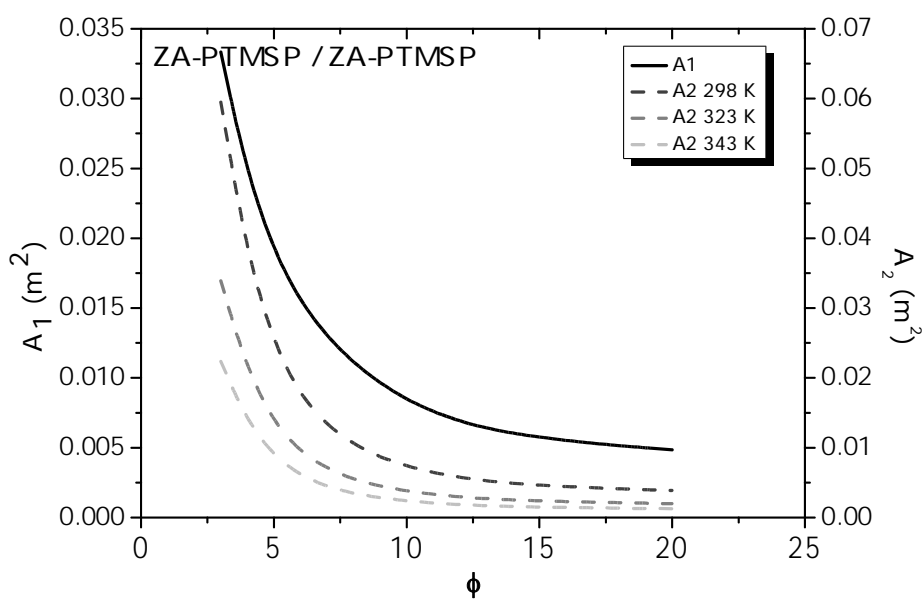
observed for the CO₂-selective Polaris® membrane, whose selectivity is in the range 12-50 [8], since the membrane separation performance is determined by the membrane properties and operating conditions.

When the ZA/PTMSP is the same membrane material used in both stages, the area required for the stage 1 doubles that of the stage 2 in all the temperature range under study, in agreement with other systems in literature [53,54]. Brinkmann et al.[55] reported that for the Polyactive ® membrane, an area of 300 m² and slightly more than 8 m² were needed in stage 1 and stage 2, which was enabled by using different types of module configuration in each stage to separate CO₂ from flue gas. Hussain and Hägg [45] analyzed an inlet stream with 700 MMSCFD, 10 % CO₂, with pressure ratios of 100 and 80 for stage 1 and stage 2, respectively, and concluded that the effective area of membrane 1 and 2 should be should be $8.20 \cdot 10^5$ m² and $2.32 \cdot 10^5$ m² in the first and the second membrane module, even for a CO₂/N₂ selectivity of 200. In this work, when the two stages are operated with different membrane materials and temperatures, 298 K and 343 K in stage 1 and stage 2, respectively, the required membrane area in stage 2 (IL-CS – Zeolite A/PTMSP and Pervap 4060 – Zeolite A/PTMSP configurations, in this work), dominates the total membrane area of the system. The reason may be that ZA/PTMSP MMM is the membrane material with the highest CO₂/N₂ separation and permeation flux, and its high thermal stability allows increasing the operating temperature in stage 2 without losing permselectivity. Figure 8 shows that this increase from 298 K to 343 K reduces the membrane area of stage 2 to a 67 % in the, ZA/PTMSP –ZA/PTMSP and Pervap 4060 – ZA/PTMSP, respectively, without the need of intermediate compressor or final vacuum [41]. It should be remarked that the use of the hybrid IL-CS membrane in stage 1 is able to reduce the influence of temperature even on the ZA/PTMSP MMM performance in stage 2, as plotted in Figure 8(a). This results reflects the translation of

the negligible influence of temperature on the ideal CO_2/N_2 selectivity through IL-CS hybrid membrane material [30] to a separation process performance.



(a)



(b)

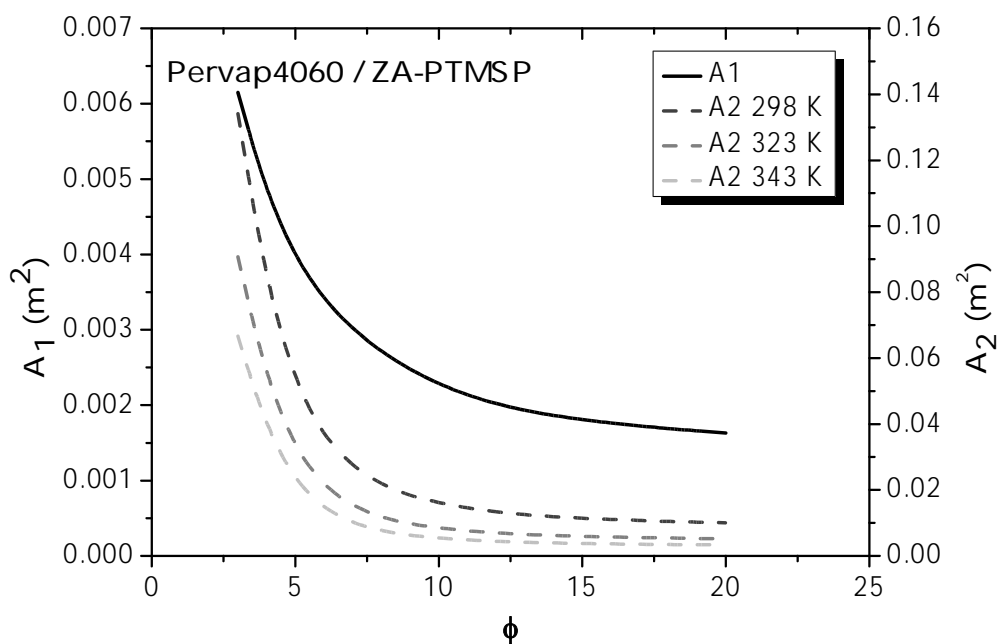


Figure 8. Analysis of the membrane area required of the membrane materials in stage 1 and stage 2, as a function of the global pressure ratio and the temperature in stage 2 for the system configurations studied. Membrane in stage 1 operates at 298 K.

Thus, to obtain 90% permeate concentration in CO₂ and 90% CO₂ removal efficiency, the membrane area in the stage 1 should be 39, 22 and 4 times that at laboratory scale, for the IL-CS – ZA/PTMSP, ZA /PTMSP – ZA/PTMSP and Pervap 4060 – ZA/PTMSP system configurations, respectively. The membrane area of the necessary ZA/PTMSP membrane at stage 2 should be 279 ± 4 times the lab-scale membrane, both at 298 K and 343 K, for the IL-CS – ZA/PTMSP system, 39 and 15 times the lab-scale membrane, for the ZA/PTMSP – ZA/PTMSP system and 87 and 43 times the lab-scale membrane for the Pervap 4060 – ZA/PTMSP system.

The CO₂ purity of the permeate is enhanced with increasing operating temperature in the stage 2 (not shown), due to the positive activation energies for CO₂ permeability of the ZA/PTMSP MMM used in stage 2 (Table 4) because the CO₂/N₂ selectivity of the ZA/PTMSP MMM is higher than those of the others [32]. By placing a high permeability and selectivity membrane material in stage 2, it is possible to increase the CO₂ purity in the permeate even at low CO₂ concentration in the feed (*i.e.*, 10%), instead of increasing the pressure ratio [56]. Besides, this makes the use of a compressor between the stages unnecessary [57].

Likewise, operating at high temperature in the stage 2 with a highly permselective membrane material, the required area to reach the 90% separation targets is reduced. From the system configurations studied in this work, the one that requires the least total membrane area to reach the 90% purity and removal efficiencies targets, is that of Pervap 4060 at stage 1 and ambient temperature and ZA/PTMSP MMM at 343 K at stage 2. For a removal efficiency of 70%, however, the membrane area required in stage 1 and stage 2 would be only 291 and 18 cm², for the ZA/PTMSP – ZA/PTMSP system, 54 and 22 cm², for the Pervap 4060 – ZA/PTMSP system, and 721 and 41 cm², for the IL-CS – ZA/PTMSP system, respectively, with CO₂ removal efficiencies in the range 89 – 95%, 87 – 94% and 80 – 90%, respectively. These values give scope to the further development and scalability of novel CO₂-selective membrane materials for carbon capture processes.

4. Conclusions

The experimental evaluation of the binary CO₂-N₂ separation performance using a two-stage membrane system with two different membranes in series has been carried out to see whether a high permeation flux in stage 1 and high permeation and selectivity

in stage 2, can lead to acceptable CO₂ removal efficiency and CO₂ concentration in the permeate, as design targets, avoiding the use of intermediate compressor or vacuum simultaneously, as well as introducing novel mixed matrix membrane materials in gas separation. When the system is fed with a CO₂ content of 10 %, the permeate is enriched to a CO₂ concentration from 26 to 43 % with a global removal efficiency up to 13% with the Pervap 4060 membrane in stage 1. The final permeate is enriched to 26, 43 and 40 % when the membrane in the first stage is IL-CS, ZA/PTMSP or Pervap 4060, respectively. The CO₂ removal efficiency of stage 2 is 49 and 64% for the IL-CS – ZA/PTMSP and Pervap 4060 – ZA/PTMSP systems. These experimental data agree well with a mathematical model, as a function of the membrane material and temperature in stage 2, for each two-stage system combination, at low CO₂ concentration in the feed.

Applying this model, we can estimate that, to attain a 90% CO₂ purity and removal efficiency at the exit, the lowest total membrane area required is obtained for the Pervap 4060 – ZA - PTMSP system, although the agreement is the worst. When the CO₂ removal efficiency is set to a lower target like 70%, the membrane area that would have to be fabricated so that these materials reach the goal in the experimental conditions of this work, would be only 291 and 18 cm² for ZA/PTMSP in stage 1 and stage 2, and 721 and 41 cm² for IL-CS and ZA/PTMSP in stage 1 and stage 2, and 54 and 22 cm² for Pervap 4060 and ZA/PTMSP for stage 1 and stage 2, respectively. These values of area are really feasible, thus giving scope to pursue the research and development of novel robust membrane materials and their potential in CO₂ capture processes. Since we have observed that the permeability and selectivity of this novel membrane materials are not greatly affected by the reduction in thickness in composite

membranes [58], we can expect an improvement of the performance. Further work on the effect of impurities such as water vapor is being conducted in our group.

Appendix

A. Mathematical model

The applied mathematical model used in this work is composed of a set of equations implemented using two different models: one covering the equations governing the membrane in stage 1 and the other used to describe the membrane in stage 2. As the permeate stream of the first stage feeds the second one, both models are connected by means of port and stream types. All the set of equations are solved using the software Aspen Custom Modeler by AspenTech®.

The overall mass balance and the component mass balance are carried out for each stage in Figure A.1, considering x_{22} as y_1 , so that the permeate stream of the stage 1 is the feed to stage 2. Since the gas separation performance depends on the membrane material, gas components in the mixture and the process conditions, the governing flux equation for the gas permeation mechanism follows Fick's law, where the driving force is the difference in partial pressures over the membrane:

$$\frac{q_{p,i}}{A_j} = \frac{q_p \cdot y_{p,i}}{A_j} = J_i = \frac{P_i}{\delta} (p_f \cdot x_f - p_p \cdot y) \quad (\text{A.1})$$

where J ($\text{m}^3(\text{STP})/\text{m}^2 \text{ h}$) is the flux of gas component i , q_p is the volumetric flow rate of the permeating gas i ($\text{m}^3(\text{STP})/\text{h}$), P_i is the intrinsic permeability of the membrane material for gas ($i = \text{CO}_2$ or N_2) ($\text{m}^3(\text{STP}) \cdot \text{m}/\text{m}^2 \text{ h bar}$), A_j is the effective membrane area (m^2) of stage j ($j = 1, 2$), δ the membrane thickness (m), p_f and p_p the pressure in the feed and permeate side, respectively, and x_f and y the molar fractions of the desired component in the feed and permeate side, respectively.

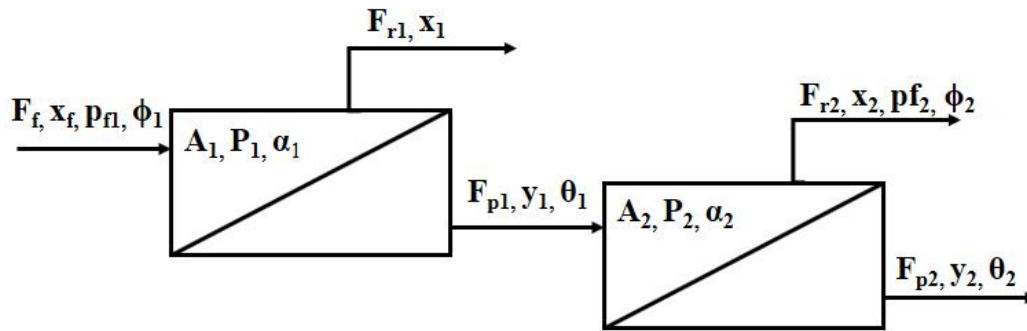


Figure A.1. Schematic diagram of the two step membrane system used in this work. Symbols are described in Appendix B.

In order to account the particularity of the experimental system validated in this work, the i component flow across the membrane in Eq. (A.1) can only occur if the partial pressure of i on the feed side of the membrane ($p_{fj} \cdot x_{fj}$) is greater than the partial pressure of i on the permeate side ($p_{pj} \cdot y_j$) [21,59]. Consequently, the maximum separation reached by the membrane cannot exceed the pressure ratio (ϕ), regardless the selectivity of the membrane [22], as mentioned before:

$$\frac{y_j}{x_{fj}} \leq \frac{p_{fj}}{p_{pj}} \rightarrow \frac{y_j}{x_{fj}} \leq \phi_j \quad (\text{A.2})$$

This is related to the different strategies possible in membrane technology are present here so that two limiting cases to be considered. On one stage, the membrane ideal selectivity is greater than the pressure ratio (ϕ), the performance is determined only by the pressure ratio across the membrane and independent of the membrane selectivity, i.e. the *pressure ratio limited region*. On the other stage, the membrane selectivity may be smaller than the pressure ratio, which is named as the *membrane*

selectivity limited region, the membrane separation is determined only by the membrane selectivity and independent of the pressure ratio [59], as in Eq. (A.3)

$$y_j = \frac{\alpha_j \cdot x_{fj}}{1 - x_{fj} \cdot (1 - \alpha_j)} \quad (\text{A.3})$$

The flow rate of the different gases passing through the membrane has to be evaluated. Eq. (A.4) describes the CO₂ transport as function of the membrane area.

When $F_{t2}=F_{p1}$,

$$\theta_j \cdot y_j = P_j \cdot \left(\frac{A_j}{F_{fj}} \right) \cdot p_{fj} \cdot \left(x_j - \left(\frac{y_j}{\phi_j} \right) \cdot \left(\frac{F_{pj}}{(F_{pj} + F_{dj})} \right) \right) \quad (\text{A.4})$$

where P_j is the CO₂ permeability, F_{fj} the feed flow and p_{fj} the pressure of the feed stream.

For a given feed flow rate and feed composition, the membrane properties (permeability and selectivity), effective membrane area, and fixed operating conditions such as pressures, pressure ratios and temperature of each stage are fixed as design parameters and the solution of system equations provides the overall performance in terms of the CO₂ purity and the recovery in the final permeate stream.

B. List of Symbols

Table B.1. Variables used in the mathematical equations.

Variable description	Units	Symbols
Input variables		
CO ₂ feed molar fraction	-	x_{fj}
Feed pressure (experimentally obtained from	bar	p_{fj}

Variable description	Units	Symbols
backpressure regulator (2) in Figure 1)		
Permeate pressure (experimentally obtained from pressure gauge (3))	bar	p_{pj}
Pressure ratio	-	Φ_j
Feed flow rate (experimentally obtained from mass flow controllers (1) in Fig. 1)	$\text{mol}\cdot\text{s}^{-1}$	F_{fj}
Permeate flow rate (experimentally obtained from flowmeter (6) in Fig. 1)	$\text{mol}\cdot\text{s}^{-1}$	F_{pj}
Dilution flow rate (measured in mass flow controller (1) in Figure 1)	$\text{mol}\cdot\text{s}^{-1}$	F_d
Output variables		
CO ₂ permeate molar fraction (experimentally obtained from gas analyzer (7) in Figure 1)	-	y_j
CO ₂ retentate molar fraction (set in mass flow controllers (1) in Figure 1)	-	x_j
CO ₂ removal efficiency	-	e
Flow rates ratio	-	$\theta_{j= F_{pj}/F_{fj}}$

$j =$ stage 1 or 2, respectively.

Table B.2. Other symbols appearing in the text and equations.

Description	Units	Symbols
Other variables		
Area	m^2	A

Description	Units	Symbols
Permeability	$\text{m}^3(\text{STP})/\text{m}^2 \text{ h bar}$	P
Solubility	$\text{cm}^3(\text{STP}) \cdot \text{cm}/\text{cm}^2 \cdot \text{s} \cdot \text{cmHg}$	S
Diffusivity	cm^2/s	D
Selectivity	-	α
Activation energy	kJ/mol	E_a
Thickness	m	δ
Temperature	K	T
Flux	$\text{m}^3(\text{STP})/\text{m}^2 \text{ h}$	J
Volumetric flow rate of the permeating gas	$\text{m}^3(\text{STP})/\text{h}$	q_p
Acronyms		
Poly(trimethyl-1-silylpropyne)	-	PTMSP
Mixed matrix membranes	-	MMM
Zeolite 4A	-	ZA
Poly(dimethylsiloxane)	-	PDMS
Ionic liquid	-	IL
Chitosan	-	CS

5. Acknowledgments

This work is partially based on a concept from Eliot S. Gerber (U.S.A.), for which he is gratefully acknowledged. The authors are also grateful for the financial support from the Spanish Ministry of Economy and Competitiveness (MINECO) under project CTQ2012-31229. A.F.B. and C.C.C. also thank the MINECO for the Early Stage

Researcher (BES2013-064266) and “Ramón y Cajal” (RYC2011-0855) contracts, respectively.

6. References

- [1] SETIS, Carbon Capture, Use and Storage, Carbon Dioxide Capture Storage Eur. Ind. Initiat. (2014) 1–5. <http://decarboni.se/publications/carbon-capture-use-and-storage-legal-resource-net> (accessed May 10, 2017).
- [2] T. Kuramochi, A. Ramírez, W. Turkenburg, A. Faaij, Comparative assessment of CO₂ capture technologies for carbon-intensive industrial processes, *Prog. Energy Combust. Sci.* 38 (2012) 87–112. doi:10.1016/j.pecs.2011.05.001.
- [3] O. de Queiroz Fernandes Araújo, J.L. de Medeiros, Carbon capture and storage technologies: present scenario and drivers of innovation, *Curr. Opin. Chem. Eng.* 17 (2017) 22–34. doi:<https://doi.org/10.1016/j.coche.2017.05.004>.
- [4] L. Gomez-Coma, A. Garea, J.C. Rouch, T. Savart, J.F. Lahitte, J.C. Remigy, A. Irabien, Membrane modules for CO₂ capture based on PVDF hollow fibers with ionic liquids immobilized, *J. Memb. Sci.* 498 (2016) 218–226. doi:10.1016/j.memsci.2015.10.023.
- [5] M. Wang, A.S. Joel, C. Ramshaw, D. Eimer, N.M. Musa, Process intensification for post-combustion CO₂ capture with chemical absorption: A critical review, *Appl. Energy.* 158 (2015) 275–291. doi:10.1016/j.apenergy.2015.08.083.
- [6] E. Chabanon, R. Bounaceur, C. Castel, S. Rode, D. Roizard, E. Favre, Pushing the limits of intensified CO₂ post-combustion capture by gas-liquid absorption

- through a membrane contactor, *Chem. Eng. Process. Process Intensif.* 91 (2015) 7–22. doi:10.1016/j.cep.2015.03.002.
- [7] C.A. Scholes, J. Bacus, G.Q. Chen, W.X. Tao, G. Li, A. Qader, G.W. Stevens, S.E. Kentish, Pilot plant performance of rubbery polymeric membranes for carbon dioxide separation from syngas, *J. Memb. Sci.* 389 (2012) 470–477. doi:10.1016/j.memsci.2011.11.011.
- [8] H. Lin, Z. He, Z. Sun, J. Vu, A. Ng, M. Mohammed, J. Knief, T.C. Merkel, T. Wu, R.C. Lambrecht, CO₂-selective membranes for hydrogen production and CO₂ capture - Part I: Membrane development, *J. Memb. Sci.* 457 (2014) 149–161. doi:10.1016/j.memsci.2014.01.020.
- [9] J. Pohlmann, M. Bram, K. Wilkner, T. Brinkmann, Pilot scale separation of CO₂ from power plant flue gases by membrane technology, *Int. J. Greenh. Gas Control.* 53 (2016) 56–64. doi:10.1016/j.ijggc.2016.07.033.
- [10] S. Roussanaly, R. Anantharaman, K. Lindqvist, H. Zhai, E. Rubin, Membrane properties required for post-combustion CO₂ capture at coal-fired power plants, *J. Memb. Sci.* 511 (2016) 250–264. doi:10.1016/j.memsci.2016.03.035.
- [11] P. Gabrielli, M. Gazzani, M. Mazzotti, On the optimal design of membrane-based gas separation processes, *J. Memb. Sci.* 526 (2016) 118–130. doi:http://dx.doi.org/10.1016/j.memsci.2016.11.022.
- [12] N.C. Mat, G.G. Lipscomb, Membrane process optimization for carbon capture, *Int. J. Greenh. Gas Control.* 62 (2017) 1–12. doi:10.1016/j.ijggc.2017.04.002.
- [13] L.M. Robeson, The upper bound revisited, *J. Memb. Sci.* 320 (2008) 390–400.

doi:10.1016/j.memsci.2008.04.030.

- [14] L.M. Robeson, *Polymer Blends in Membrane Transport Processes*, *Ind. Eng. Chem. Res.* 49 (2010) 11859–11865.
- [15] J.C. Abanades, B. Arias, A. Lyngfelt, T. Mattisson, D.E. Wiley, H. Li, M.T. Ho, E. Mangano, S. Brandani, *Emerging CO₂ capture systems*, *Int. J. Greenh. Gas Control.* 40 (2015) 126–166. doi:10.1016/j.ijggc.2015.04.018.
- [16] A.M. Arias, M.C. Mussati, P.L. Mores, N.J. Scenna, J.A. Caballero, S.F. Mussati, *Optimization of multi-stage membrane systems for CO₂ capture from flue gas*, *Int. J. Greenh. Gas Control.* 53 (2016) 371–390. doi:10.1016/j.ijggc.2016.08.005.
- [17] R. Khalilpour, K. Mumford, H. Zhai, A. Abbas, G. Stevens, E.S. Rubin, *Membrane-based carbon capture from flue gas: A review*, *J. Clean. Prod.* 103 (2015) 286–300. doi:10.1016/j.jclepro.2014.10.050.
- [18] X. He, M.B. Hägg, *Hollow fiber carbon membranes: Investigations for CO₂ capture*, *J. Memb. Sci.* 378 (2011) 1–9. doi:10.1016/j.memsci.2010.10.070.
- [19] K. Ramasubramanian, H. Verweij, W.S. Winston Ho, *Membrane processes for carbon capture from coal-fired power plant flue gas: A modeling and cost study*, *J. Memb. Sci.* 421–422 (2012) 299–310. doi:10.1016/j.memsci.2012.07.029.
- [20] L. Zhao, E. Riensche, M. Weber, D. Stolten, *Cascaded Membrane Processes for Post-Combustion CO₂ Capture*, *Chem. Eng. Technol.* 35 (2012) 489–496. doi:10.1002/ceat.201100462.
- [21] T.C. Merkel, H. Lin, X. Wei, R. Baker, *Power plant post-combustion carbon*

- dioxide capture: An opportunity for membranes, *J. Memb. Sci.* 359 (2010) 126–139. doi:10.1016/j.memsci.2009.10.041.
- [22] Y. Huang, T.C. Merkel, R.W. Baker, Pressure ratio and its impact on membrane gas separation processes, *J. Memb. Sci.* 463 (2014) 33–40. doi:10.1016/j.memsci.2014.03.016.
- [23] T.C. Merkel, X. Wei, Z. He, L.S. White, J.G. Wijmans, R.W. Baker, Selective Exhaust Gas Recycle with Membranes for CO₂ Capture from Natural Gas Combined Cycle Power Plants, *Ind. Eng. Chem. Res.* 52 (2013) 1150–1159. doi:10.1021/ie302110z.
- [24] Z. Yuan, M.R. Eden, R. Gani, Toward the Development and Deployment of Large-Scale Carbon Dioxide Capture and Conversion Processes, *Ind. Eng. Chem. Res.* 55 (2016) 3383–3419. doi:10.1021/acs.iecr.5b03277.
- [25] E. Gerber, Production of electric power from fossil fuel with almost zero air pollution, WO2015076859A1, 2015.
- [26] A. Brunetti, Y. Sun, A. Caravella, E. Drioli, G. Barbieri, Process intensification for greenhouse gas separation from biogas: More efficient process schemes based on membrane-integrated systems, *Int. J. Greenh. Gas Control.* 35 (2015) 18–29. doi:10.1016/j.ijggc.2015.01.021.
- [27] A.S. Bhowan, Status and analysis of next generation post-combustion CO₂ capture technologies, *Energy Procedia.* 63 (2014) 542–549. doi:10.1016/j.egypro.2014.11.059.
- [28] K. Lindqvist, S. Roussanaly, R. Anantharaman, Multi-stage membrane processes

- for CO₂ capture from cement industry, in: *Energy Procedia*, 2014: pp. 6476–6483. doi:10.1016/j.egypro.2014.11.683.
- [29] R. Koc, N.K. Kazantzis, Y.H. Ma, Membrane technology embedded into IGCC plants with CO₂ capture: An economic performance evaluation under uncertainty, *Int. J. Greenh. Gas Control*. 26 (2014) 22–38. doi:10.1016/j.ijggc.2014.04.004.
- [30] E. Santos, E. Rodríguez-Fernández, C. Casado-Coterillo, A. Irabien, Hybrid ionic liquid-chitosan membranes for CO₂ separation: Mechanical and thermal behavior, *Int. J. Chem. React. Eng.* 14 (2016) 713–718. doi:10.1515/ijcre-2014-0109.
- [31] A. Fernández-Barquín, C. Casado-Coterillo, M. Palomino, S. Valencia, A. Irabien, LTA/Poly(1-trimethylsilyl-1-propyne) Mixed-Matrix Membranes for High-Temperature CO₂/N₂ Separation, *Chem. Eng. Technol.* 38 (2015) 658–666. doi:10.1002/ceat.201400641.
- [32] A. Fernández-Barquín, C. Casado-Coterillo, M. Palomino, S. Valencia, A. Irabien, Permselectivity improvement in membranes for CO₂/N₂ separation, *Sep. Purif. Technol.* 157 (2016) 102–111. doi:10.1016/j.seppur.2015.11.032.
- [33] F. Ahmad, K.K. Lau, A.M. Shariff, G. Murshid, Process simulation and optimal design of membrane separation system for CO₂ capture from natural gas, *Comput. Chem. Eng.* 36 (2012) 119–128. doi:10.1016/j.compchemeng.2011.08.002.
- [34] J.P. Van-der-Slujis, C.A. Hendriks, K. Blok, Feasibility of polymer membranes for carbon dioxide recovery from flue gas, *Energy Convers. Manag.* 33 (1992) 429–436.

- [35] M. Binns, S. Lee, Y.-K. Yeo, J.H. Lee, J.-H. Moon, J. Yeo, J.-K. Kim, Strategies for the simulation of multi-component hollow fibre multi-stage membrane gas separation systems, *J. Memb. Sci.* 497 (2016) 458–471. doi:10.1016/j.memsci.2015.08.023.
- [36] S.S.M. Lock, K.K. Lau, F. Ahmad, A.M. Shariff, Modeling, simulation and economic analysis of CO₂ capture from natural gas using cocurrent, countercurrent and radial crossflow hollow fiber membrane, *Int. J. Greenh. Gas Control*. 36 (2015) 114–134. doi:10.1016/j.ijggc.2015.02.014.
- [37] R. Qi, M.A. Henson, Optimal design of spiral-wound membrane networks for gas separations, *J. Memb. Sci.* 148 (1998) 71–89. doi:10.1016/S0376-7388(98)00143-4.
- [38] M.H. Murad Chowdhury, X. Feng, P. Douglas, E. Croiset, A new numerical approach for a detailed multicomponent gas separation membrane model and AspenPlus simulation, *Chem. Eng. Technol.* 28 (2005) 773–782. doi:10.1002/ceat.200500077.
- [39] M.J. Thundyil, Y.H. Jois, W.J. Koros, Effect of permeate pressure on the mixed gas permeation of carbon dioxide and methane in a glassy polyimide, *J. Memb. Sci.* 152 (1999) 29–40. doi:10.1016/S0376-7388(98)00153-7.
- [40] J. Kotowicz, T. Chmielniak, K. Janusz-Szymańska, The influence of membrane CO₂ separation on the efficiency of a coal-fired power plant, *Energy*. 35 (2010) 841–850. doi:10.1016/j.energy.2009.08.008.
- [41] R. Qi, M.A. Henson, Membrane system design for multicomponent gas mixtures

- via mixed-integer nonlinear programming, *Comput. Chem. Eng.* 24 (2000) 2719–2737. doi:10.1016/S0098-1354(00)00625-6.
- [42] M. Scholz, T. Harlacher, T. Melin, M. Wessling, Modeling gas permeation by linking nonideal effects, *Ind. Eng. Chem. Res.* 52 (2013) 1079–1088. doi:10.1021/ie202689m.
- [43] F. Ahmad, K.K. Lau, A.M. Shariff, Removal of CO₂ from natural gas using membrane separation system: modeling and process design, *J. Appl. Sci.* 10 (2010) 1134–1139.
- [44] H. Lababidi, G.A. Al-Enezi, H.M. Ettouney, Optimization of module configuration in membrane gas separation, *J. Memb. Sci.* 112 (1996) 185–197. doi:10.1016/0376-7388(95)00283-9.
- [45] A. Hussain, M.-B. Hägg, A feasibility study of CO₂ capture from flue gas by a facilitated transport membrane, *J. Memb. Sci.* 359 (2010) 140–148. doi:10.1016/j.memsci.2009.11.035.
- [46] V. Sebastián, I. Kumakiri, R. Bredesen, M. Menéndez, Zeolite membrane for CO₂ removal: Operating at high pressure, *J. Memb. Sci.* 292 (2007) 92–97. doi:10.1016/j.memsci.2007.01.017.
- [47] J.S. Lee, W. Madden, W.J. Koros, Antiplasticization and plasticization of Matrimid® asymmetric hollow fiber membranes—Part A. Experimental, *J. Memb. Sci.* 350 (2010) 232–241. doi:10.1016/j.memsci.2009.12.033.
- [48] J.S. Lee, W. Madden, W.J. Koros, Antiplasticization and plasticization of Matrimid® asymmetric hollow fiber membranes. Part B. Modeling, *J. Memb.*

- Sci. 350 (2010) 242–251. doi:10.1016/j.memsci.2009.12.034.
- [49] A.F. Ismail, W. Lorna, Penetrant-induced plasticization phenomenon in glassy polymers for gas separation membrane, *Sep. Purif. Technol.* 27 (2002) 173–194. doi:10.1016/S1383-5866(01)00211-8.
- [50] T. Visser, G.H. Koops, M. Wessling, On the subtle balance between competitive sorption and plasticization effects in asymmetric hollow fiber gas separation membranes, *J. Memb. Sci.* 252 (2005) 265–277. doi:10.1016/j.memsci.2004.12.015.
- [51] C.A. Scholes, J. Jin, G.W. Stevens, S.E. Kentish, Competitive permeation of gas and water vapour in high free volume polymeric membranes, *J. Polym. Sci. Part B Polym. Phys.* 53 (2015) 719–728. doi:10.1002/polb.23689.
- [52] E. Favre, Carbon dioxide recovery from post-combustion processes: Can gas permeation membranes compete with absorption?, *J. Memb. Sci.* 294 (2007) 50–59. doi:10.1016/j.memsci.2007.02.007.
- [53] L. Zhao, E. Riensche, L. Blum, D. Stolten, Multi-stage gas separation membrane processes used in post-combustion capture: Energetic and economic analyses, *J. Memb. Sci.* 359 (2010) 160–172. doi:10.1016/j.memsci.2010.02.003.
- [54] J. Franz, S. Schiebahn, L. Zhao, E. Riensche, V. Scherer, D. Stolten, Investigating the influence of sweep gas on CO₂/N₂ membranes for post-combustion capture, *Int. J. Greenh. Gas Control.* 13 (2013) 180–190. doi:10.1016/j.ijggc.2012.12.008.
- [55] T. Brinkmann, J. Pohlmann, M. Bram, L. Zhao, A. Tota, N. Jordan Escalona, M. de Graaff, D. Stolten, Investigating the influence of the pressure distribution in a

- membrane module on the cascaded membrane system for post-combustion capture, *Int. J. Greenh. Gas Control.* 39 (2015) 194–204. doi:10.1016/j.ijggc.2015.03.010.
- [56] H. Zhai, E.S. Rubin, Techno-Economic Assessment of Polymer Membrane Systems for Postcombustion Carbon Capture at Coal-Fired Power Plants, *Environ. Sci. Technol.* 47 (2013) 3006–3014. doi:10.1021/es3050604.
- [57] M. Yuan, K. Narakornpijit, R. Haghpanah, J. Wilcox, Consideration of a nitrogen-selective membrane for postcombustion carbon capture through process modeling and optimization, *J. Memb. Sci.* 465 (2014) 177–184. doi:10.1016/j.memsci.2014.04.026.
- [58] A. Fernández-Barquín, C. Casado-Coterillo, M. Etxeberria-Benavides, J. Zuñiga, A. Irabien, Comparison of flat and hollow fiber mixed matrix composite membranes for CO₂ separation with temperature, *Chem. Eng. Technol.* 40 (2017) 997–1007. doi:10.1002/ceat.201600580.
- [59] R.W. Baker, *Membrane Technology and Applications*, 2nd ed., John Wiley & Sons, Chichester, England, 2004. doi:10.1016/S0376-7388(00)83139-7.

Highlights

- Introduction of novel mixed matrix membranes in CO₂-N₂ separation systems.
- Three cascade schemes with two different membrane types are analyzed.
- High permeability and low selectivity membrane is placed in stage 1.
- High permselectivity and thermally resistant MMM in stage 2 avoids the use of compressor.
- For a 70% CO₂ purity, affordable membrane areas are required.

ACCEPTED MANUSCRIPT